J Fluoresc (2014) 24:1263–1274
DOI 10.1007/s10895-014-1410-3

ORIGINAL PAPER

Fluorescent Coumarin Derivatives with Viscosity Sensitive Emission - Synthesis, Photophysical Properties and Computational Studies

Kiran R. Phatangare · Sandip K. Lanke · Nagaiyan Sekar

Received: 3 April 2014 / Accepted: 19 May 2014 / Published online: 3 June 2014

Abstract New derivatives of (benzo[*d*]azolyl)-benzo[*f*]-chromenone were synthesized from the intermediate 3-(1,3-benzazol-2-yl)naphthalen-2-ol, obtained from 3-hydroxynaphthalene-2-carboxylic acid and 2-amino phenol in the presence of PCl_3 in chlorobenzene at 130–135 °C. The compounds were characterized by FT-IR, ^1H NMR, mass spectroscopy and elemental analysis. The synthesized compounds are fluorescent which absorb in the range of 296 to 332 nm while emit in the range of 368 to 404 nm. The experimental absorption and emission wavelengths for the compounds 5 and 6 are in good agreement with those predicted using the Time-Dependent Density Functional Theory (TD-DFT) [B3LYP/6-31G(d)]. The largest wavelength difference between the experimental and computed absorption maxima was 29 nm (tetrahedrofuran) for compound 5 while for emission it was 61 nm (dichloromethane) for compound 7. The emission intensities of all the compounds decrease continuously as the viscosity of the microenvironment increases. The compounds are thermally stable up to a temperature range of 300 to 350 °C.

Keywords Benzoxazolylnaphthalenol · DFT · 3H-benzo[f]chromen-3-one · Fluorescence · Heterocyclic synthesis · Photophysical properties · Viscosity

Electronic supplementary material The online version of this article (doi:10.1007/s10895-014-1410-3) contains supplementary material, which is available to authorized users.

K. R. Phatangare · S. K. Lanke · N. Sekar (✉)
Department of Intermediates and Dyestuff Technology, Institute of Chemical Technology (Formerly UDCT), N. P. Marg, Matunga, Mumbai 400 019, Maharashtra, India
e-mail: n.sekar@ictmumbai.edu.in

Introduction

In recent years, research has been intensified to synthesize fluorescent heterocyclic compounds which are used as fluorescence sensors [1], molecular probes in biochemical research [2], fluorescence labeling reagents [3], fluorescent probes for different metal ions, thiols, anions [4–6] and in the traditional textile and polymer fields [7]. Specifically, those fluorescent compounds which emit in the red region play an important role in full color electroluminescence displays and in biology [8, 9]. Heterocyclic fluorescent compounds are of contemporary interest in the search for new diagnostic methods [10].

Coumarin are an elite class of fluorescent compounds present in various natural products [11–13] affording a wide range of organic materials which find use in applications where intense fluorescence is important [14–16]. Fluorescent coumarin colorants show promising photophysical and photochemical properties, reasonable stability, good solubility and relative ease of synthesis. As a result, coumarin derivatives are extensively investigated as probes for biological applications, in particular for in vivo imaging of cells in living organisms [17–19], optical brighteners [20], organic nonlinear optical materials [21–25]. They constitute the largest class of laser dyes in the 'blue–green' region [26–29]. Coumarin dyes have been used as red, green and blue dopants in organic light-emitting diodes (OLEDs) [30–32]. Coumarin derivatives have been extensively investigated for electronic and photonic applications such as solar energy collectors, charge-transfer agents [33–36].

Coumarin with an electron repelling substitution at the 7-position enhances the electron density of coumarin ring and leads to a red-shifted absorption [37–42]. However, coumarin dyes suffer from some disadvantages such as the small Stokes shift. It is intriguing to note that, coumarin dyes show typical

Stokes shift is less than 30 nm [43, 44]. It is noteworthy that the compounds with benzocoumarin skeleton which disperses the electron density of the coumarin ring, leading to blue shifted absorption with a larger Stokes shift compared to the 7-substituted counterparts are known [45]. Also the substitution of an electron acceptor group at the 8- position of the coumarin ring shows blue shifted emission as compared to the substitution at 3-position, but it shows a high Stokes shift [46]. Envisaging a large Stokes shift and higher quantum yield our interest of the current research work turned towards the design and synthesize of new 5, 6-benzofused coumarin derivatives with the acceptor groups like benzimidazole and benzoxazole at the 8-position. It is to be noted that there are a few reports are available in the literature where benzene ring is fused at 5, 6 position [47–51].

In continuation of our research work on fluorescent heterocyclic compounds [52–56] here in this paper we report the synthesis of novel fluorescent coumarin derivatives from 3-(1, 3-benzoxazol-2-yl)naphthalen-2-ol (4–7), and their photophysical properties. An extensive computation of the ground and the excited state geometries of these molecules have been carried out using Density Functional Theory (DFT) and Time Dependent Density Functional Theory (TDDFT). The experimental photophysical properties have been compared with those obtained from DFT and TDDFT Scheme 1.

Results and Discussions

Absorption and Solvatochromism Study

To evaluate the effect of solvent polarity on the absorption-emission properties of the synthesized coumarin, all the coumarin 4–7 were tested in different solvents of varying polarity and hydrogen bonding capability. Nine solvents were tested for the effect of solvent on their absorption-emission characteristics.

The solvatochromism study of the coumarin 4 states that it show two distinct absorption peaks in all the solvents irrespective of the polarity, one at 314–317 nm and the other at 329–332 nm. It shows single absorption peak in acetone (Fig. 1) with least molar absorptivity of 30,378 M^{-1} cm^{-1} as compared to the other solvents (SI-Table 1). The highest absorption intensity was observed for THF with an absorptivity of 41,202.0 M^{-1} cm^{-1}.

The largest difference in wavelength between the computed and experimental absorption maxima is 14 nm in DMF for

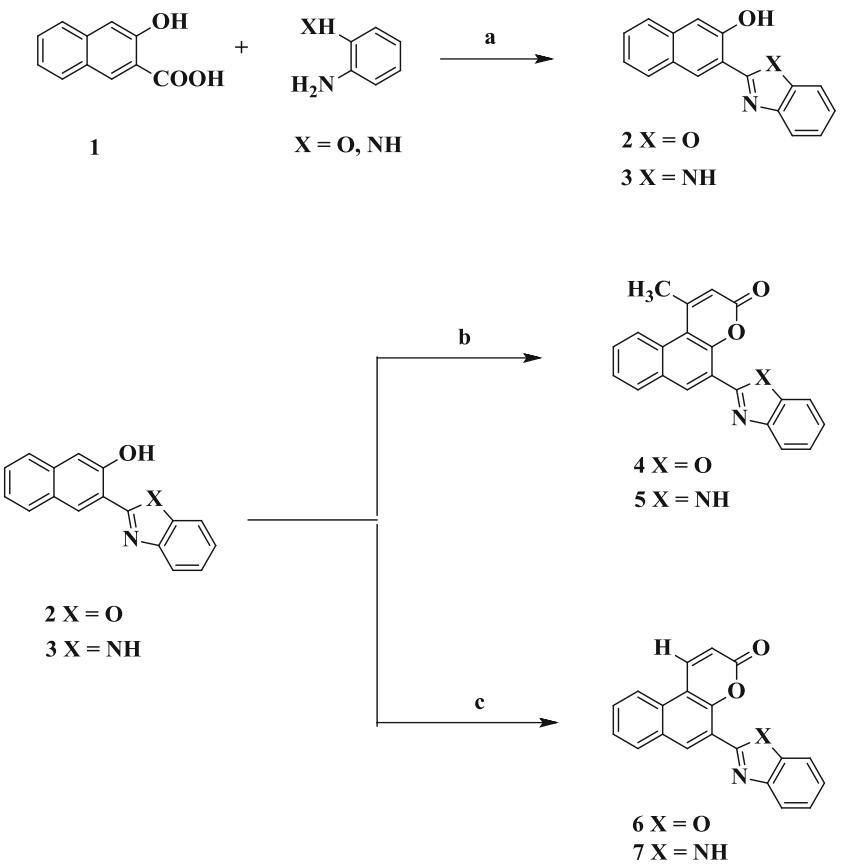

Scheme 1 Synthesis of benzoxazolyl-benzo[*f*]chromen-3-one from 3-hydroxynaphthalene-2-carboxylic acid via 3-(1,3-benzoxazol-2-yl)naphthalen-2-ol. Reagent and Conditions: **a** X=O, Chlorobenzene/PCl_3, 4 h, X=NH, PPA, 3.5 h. **b** Ethyl acetoacetate, conc. H_2SO_4, room temperature, 16 h. **c** 2-hydroxybutanedioic acid, conc. H_2SO_4, room temperature, 14 h

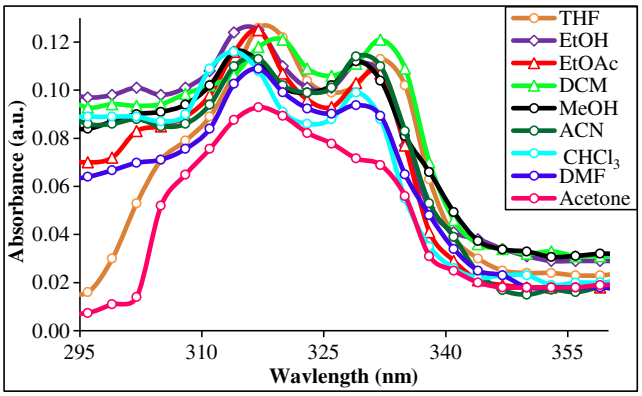

Fig. 1 Absorption spectra of coumarin 4

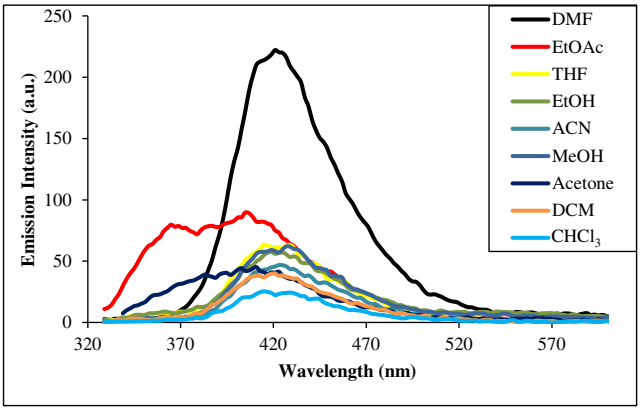

Fig. 3 Emission spectra of coumarin 4

shorter wavelength region. In case of long wavelength region it is 24 nm in $CHCl_3$. In THF the computed vertical excitation at 306 nm with oscillator strength of 0.4358 was obtained from the third excited state which corresponds to the absorption at the shorter wavelength (317 nm). The vertical excitation obtained in the second excited state at 349 nm with oscillator strength of 0.1795 corresponds to the absorption at longer wavelength (349 nm) (SI -Table 1). The vertical excitation presented in Fig. 2 for methanol solvent states that the absorption at 306 nm is because of HOMO to LUMO+1, corresponding to the experimentally observed absorption at 314 nm while the absorption at 349 nm is due HOMO-1 to LUMO transition which corresponds to the peak at 329 nm in methanol.

In all the solvents, the prominent intense absorption can be assigned to HOMO to LUMO+1 transition and the other less intense absorption arises from HOMO-1 to LUMO transition (SI-Table 1).

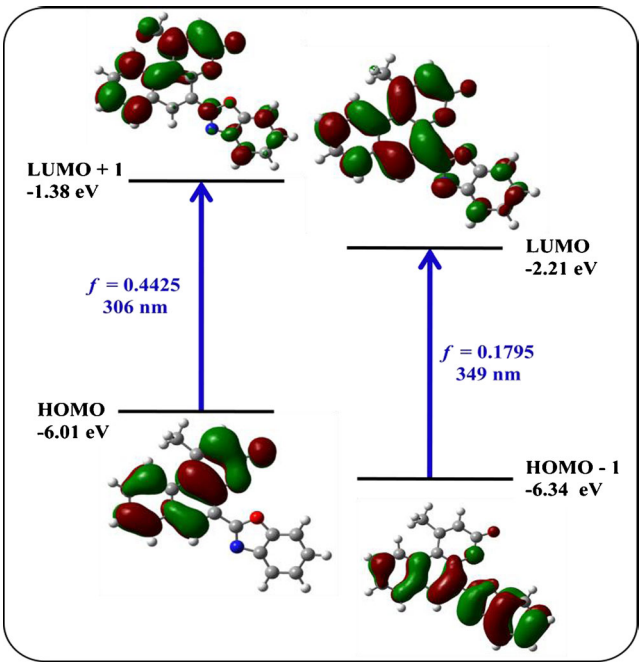

Fig. 2 Representation of the UV-visible absorption (vertical excitation) coumarin 4 in methanol.[a]

The coumarin 4 emits at 404 to 426 nm with a Stokes shift of 6,754–8,372 cm^{-1}. Methanol shows the largest Stokes shift of 8,372 cm^{-1} but the quantum yield arises from it is least in all the solvents. In DMF the coumarin shows hyperchromic shift as compared to the other solvents which is attributed to the highest quantum yield of 0.113. (Fig. 3) The quantum yield varies from 0.071 to 0.113 (Table 1).

Solvatochromism and Solvatofluorism Study of Coumarin 5

Except in acetone and THF, the coumarin 5 shows two prominent absorption peaks ranging from 317 to 332 nm. But the absorption remains same in both polar and non-polar solvents, but chloroform shows the hyperchromic effect with the highest molar absorptivity of 29,014.0 $M^{-1}.cm^{-1}$ (Fig. 4, SI-Table 2). In the case of polar solvent methanol TD-DFT computed vertical excitation from HOMO→LUMO+1 (66 %) at 309 nm with the oscillator strength of 0.5981 arises from the excited state 4 corresponding to the experimentally observed λ_{max} 317 nm (SI-Table 2).

The vertical excitation from HOMO-1→LUMO which contributes 58 % from the second excited state corresponds to the shoulder peak at 332 nm in methanol. A very similar trend was observed in all the other solvents except in chloroform wherein HOMO-1→LUMO (64 %) from the excited state corresponds to the shoulder peak at 332 nm (SI-Table 2).

The coumarin 5 absorbs in the range of 317–335 nm and emits in the range of 378 to 450 nm with the Stokes shift from 3,395 to 7,898 cm^{-1}. The largest red shift was observed in chloroform (72 nm) than in DMF (26 nm) as compared to the solvent acetone (Fig. 5). In the solvents like DMF and DCM the coumarin 7 shows hyperchromic effect attributed to the highest quantum yield of 0.189 and 0.151 respectively. The lowest quantum yield of 0.075 and 0.042 was observed in ethyl acetate and THF respectively (Table 1).

Table 1 Observed UV-visible absorption and computed absorption of coumarin 4–7 in different solvents[a]

Dye	Solvent	λ_{abs} (nm)	λ_{em} (nm)	ε ($M^{-1}.cm^{-1}$)	$\Delta\lambda$ (cm^{-1})	Φ_F[b]	TD-DFT λ_{em} (nm)
4	THF	317	414	41,202.0	7,391	0.088	403
	EtOAc	317	404	40,875.0	6,793	0.090	402
	$CHCl_3$	317	415	37,932.0	7,449	0.101	402
	DCM	317	420	39,567.0	7,736	0.084	403
	Acetone	317	411	30,378.3	7,214	0.086	405
	MeOH	314	426	37,932.0	8,372	0.071	406
	ETOH	314	418	40,548.0	7,923	0.083	406
	ACN	329	423	36,951.0	6,754	0.089	406
	DMF	320	421	35,610.3	7,497	0.110	406
5	THF	332	396	27,058.0	4,867	0.042	434
	EtOAc	317	384	26,080.0	5,504	0.075	-
	$CHCl_3$	332	450	28,036.0	7,898	0.102	437
	DCM	332	386	17,930.0	4,213	0.151	-
	Acetone	335	378	16,691.2	3,395	0.058	432
	MeOH	317	394	27,058.0	6,165	0.118	432
	EtOH	320	389	24,450.0	5,543	0.120	432
	ACN	332	398	23,080.8	4,994	0.060	432
	DMF	332	404	21,168.0	5,368	0.189	431
6	THF	317	431	50,393.0	8,343	0.057	405
	EtOAc	317	427	38,499.0	8,126	0.033	404
	$CHCl_3$	317	408	23,162.0	7,035	0.036	403
	DCM	317	423	37,560.0	7,905	0.035	405
	Acetone	335	411	19,719.0	5,519	0.019	407
	MeOH	317	438	26,605.0	8,714	0.144	407
	EtOH	317	435	25,666.0	8,557	0.120	407
	ACN	329	405	18,154.0	5,703	0.041	407
	DMF	317	435	20,814.5	8,557	0.092	407
7	THF	324	398	12,480.0	5,738	0.069	440
	EtOAc	318	384	22,152.0	5,404	0.040	441
	$CHCl_3$	321	442	42,432.0	8,528	0.061	443
	DCM	333	378	20,904.0	3,575	0.119	439
	Acetone	339	390	21,996.0	3,857	0.055	437
	MeOH	336	396	12,480.0	4,509	0.154	436
	EtOH	315	412	20,592.0	7,474	0.082	436
	ACN	330	394	17,160.0	4,922	0.069	436
	DMF	333	408	19,344.0	5,520	0.140	436

[a] Analysis were carried out at room temperature (25 °C); [b] Tinopal was used as reference standard for quantum yield calculations

Solvatochromism and Solvatofluorism Study of Coumarin 6

Except in the solvents acetonitrile and acetone the coumarin 6 shows two distinct absorption peaks, one major absorption maxima at 317 nm while the shoulder peak at 329 to 335 nm (Fig. 6). The solvents acetonitrile and acetone show the absorption maxima at 329 and 335 nm. The highest molar absorptivity of 50,393.0 M^{-1} cm^{-1} was obsereved in THF while the least value was observed in acetonitrile (18,154.0 M^{-1} cm^{-1}).

The largest difference in the computed and experimental absorption for the coumarin 6 was 5 nm in ethyl acetate for shorter wavelength absorption and 29 nm in THF for longer wavelength absorption. The vertical excitations HOMO→LUMO+1 (66-67 %) with the highest oscillator strength of 0.5065 - 0.5288 are presented in (SI-Table 3) are from the third excited state for all the solvents which correspond to the experimentally observed absorption λ_{max} at 317 nm. The vertical excitation HOMO-1→LUMO (67 %) from the second excited state (oscillator strength (*f*)=0.1370–0.1496)

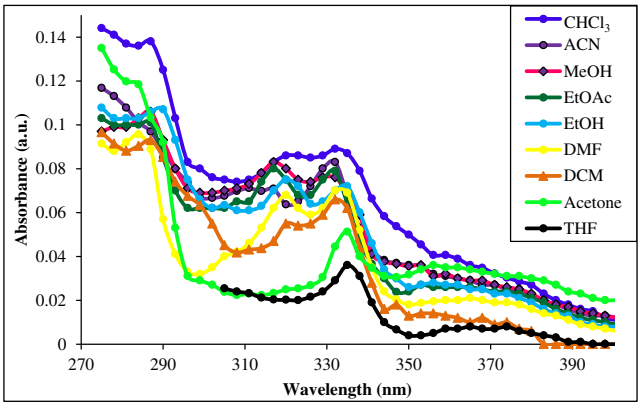

Fig. 4 Absorption spectra of coumarin 5

corresponds to the experimentally observed shoulder peak at 329–335 nm (SI-Table 3).

The coumarin 6 emits in the range of 405 to 438 nm with Stokes shift from 5,519 to 8,714 cm^{-1} (Table 1). In the solvents acetonitrile and chloroform the coumarin 6 emits at 405 and 408 nm respectively which is slightly blue shifted than in methanol and DMF (Fig. 7). In methanol and ethanol the highest emission intensity was observed which is attributed to the highest quantum yield of 0.144 and 0.120 respectively. The least quantum yield was observed in acetone (Φ= 0.019) as its emission intensity is very poor (Table 1).

Solvatochromism and Solvatofluorism Study of Coumarin 7

In the non-polar solvent like chloroform and THF the coumarin 7 shows hyperchromic shift in absorption while reverse is the case in the polar solvent (hypochromic effect) (Fig. 8). In these two solvents it shows one major peak (321 and 324 nm) and the other shoulder peak at 330 and 348 nm while for other solvent both the peaks are of equal intensity. The highest molar absorptivity of 42,432.0 M^{-1} cm^{-1} was observed for chloroform (SI-Table 4).

The largest difference between the computed and the experimental absorption is 7 nm and 23 nm respectively in

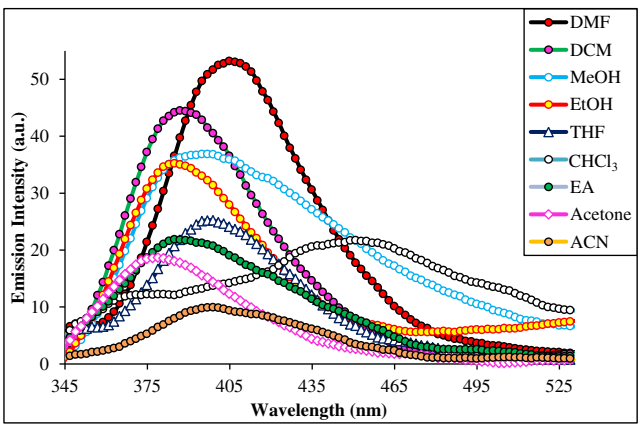

Fig. 5 Emission spectra of coumarin 5

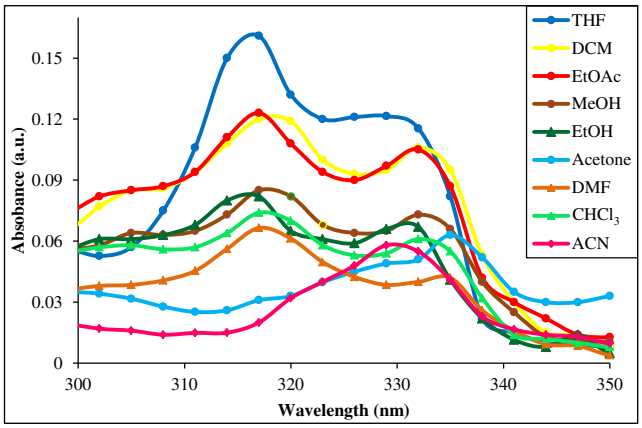

Fig. 6 Absorption spectra of coumarin 6

ethanol and acetonitrile for the long wavelength absorption. The HOMO→LUMO+1 vertical excitation with a contribution of 67 % and oscillator strength of 0.5815 corresponds the to the experimental absorption maxima at 321 nm. This contribution arises from the fourth excited state. From the third excited state HOMO-2→LUMO transition with a contribution of 49 % corresponds to the shoulder peak at 336 nm in methanol. Similar trend was observed for the other solvents except chloroform and ethyl acetate. In these two solvents HOMO-2→LUMO transition from the third excited state corresponds to the experimentally observed shoulder peak at 351 and 330 nm respectively (SI-Table 4).

In chloroform the coumarin 7 shows 64 nm red shift as compared to DCM with the largest Stokes shift but the quantum yield was less as compared with the other solvents as its emission intensity is less Fig. 9. It emits in the range of 378 to 442 nm with a Stokes shift of 3,575 to 8,528 cm^{-1}. The highest quantum yield of 0.154 and 0.140 was observed in methanol and DMF. For the other solvents it varies from 0.040 to 0.119 (Table 1).

Figure 10 and 11 represents the daylight and UV light photographs of coumarin 4–7.

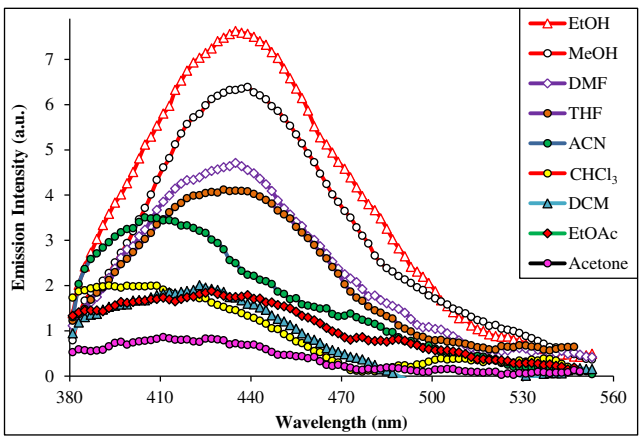

Fig. 7 Emission spectra of coumarin 6

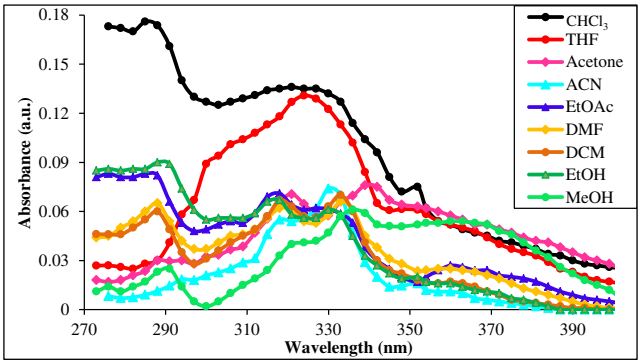

Fig. 8 Absorption spectra of coumarin 7

Effect of Viscosity on Absorption of Coumarin 4–7

Viscosity has a great impact on the fluorescence intensity. All the synthesized coumarin 4–7 were studied for their effect of viscosity on absorption as well as emission intensity. The absorption intensity is in the case of all the coumarin 4–7. Exceptionally there is a slight decrease in the absorption intensity in the case of the coumarin 7 (Fig. 12).

In the case of the emission viscosity show interesting results and are predictable. For all the coumarin 4–7 emission peak intensity goes on decreasing as viscosity increases (Figs. 13 and 14).

Structural Parameters

There are two possible rotamers for each compound. In 'rotamer a' the pending benzazole ring nitrogen is closer towards chromone oxygen while in 'rotamer b' benzoyl oxygen is closer to the chromone oxygen (Fig. 15). The Table 2 for ground state stability of each coumarin 4–7 states that the 'rotamer b' for all coumarin 4–7 is more stable than the 'rotamer a'. The 'rotamer b' for all the coumarin 4–7 was optimized in nine different solvents and their optimized structures in methanol are presented in Fig. 16. The dihedral angle C9-C8-C15-O19 is zero for all rotamers except 4b and 5b. It is 27.97° and −1.22° for rotamer 4b and 5b.

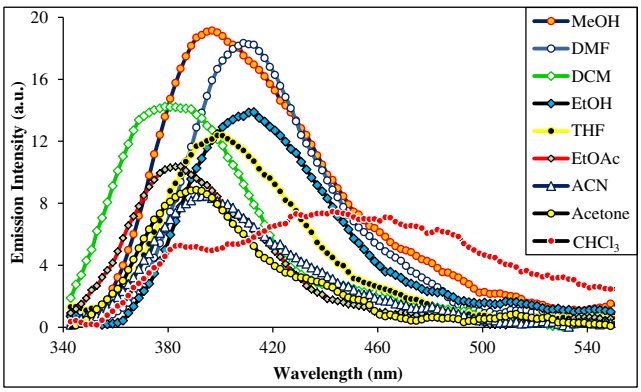

Fig. 9 Emission spectra of coumarin 7

Day light photograph

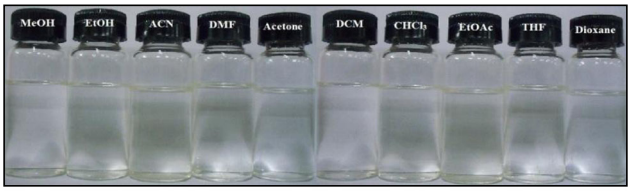

UV light photograph

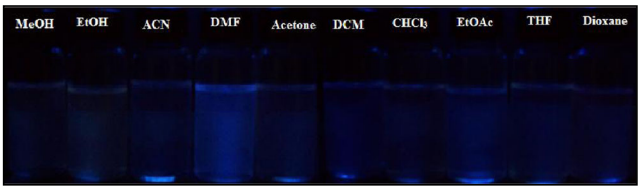

Fig. 10 Daylight and UV light photographs of coumarin 4

The angle C12-O11-C9 is 123.6° which are slightly less than that of in other rotamers. The bond distance C15-O19 in rotamers 4b and 6b are 1.374 Å and 1.373 Å respectively while C18–C19 bond distances are same in both the rotamers (1.372 Å) (Fig. 16). The C15-N19 and N19-C18 bond distances in rotamers 5b and 7b are 1.377 Å and 1.378 Å respectively (Fig. 16).

Thermogravimetric Analysis

To investigate the thermal stability of the synthesized coumarin 4–7, thermal stability study has been carried out using thermo gravimetric analysis (TGA) technique. The thermal gravimetric analysis has been carried out over the temperature range of 50–600 ºC under nitrogen atmosphere. TGA result in (SI-Table 5) indicates that the stability of all compounds varies from 302 to 349 ºC. All the compounds start to decompose in between 302 and 368 ºC. TGA analysis curves of all the coumarin (4–7) as shown in Fig. 17 state that even up to 400 ºC the coumarin 6 is stable up to 74.83 %. The coumarin 7 almost decomposes 75–80 % up to 450 ºC. None of the coumarin decomposes completely up to 600 ºC. The comparison of T_d (decomposition temperature) showed that the thermal stability of the coumarin 4–7 decreases in the order 6>7>5>4 as shown in (SI-Table 5).

Experimental Sections

Materials and Methods

All the commercial reagents were purchased and used without purification and all the solvents were of reagent grade. The reaction was monitored by TLC using on 0.25 mm silica gel 60 F254 precoated plates, which were visualized with UV light. Melting points were measured on standard melting point

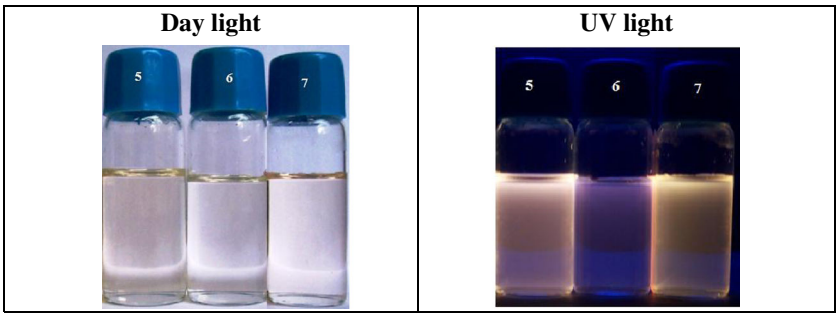

Fig. 11 Daylight and UV light photographs of coumarin 5–7 in DMF

apparatus and are uncorrected. The FT-IR spectra were recorded on a Fourier Transform IR instrument (ATR accessories). ^{1}H NMR and ^{13}C NMR spectra were recorded on NMR spectrometer operating at 300 MHz and 75 MHz respectively using TMS as an internal standard. Mass spectra were recorded on mass spectrometer instrument. The absorption spectra of the compounds were recorded on UV-visible spectrophotometer; fluorescence emission spectra were recorded on fluorescence spectrophotometer using freshly prepared solutions. Quantum yield was calculated by using tinopal (Φ=0.81 in DMF) [57, 58].

Computational Methods

The different conformers of the coumarin 4 to 7 and their tautomers involved are illustrated in Fig. 2. The ground state (S_o) geometry of the conformers and tautomers of all these compounds in their C_s symmetry were optimized in the gas phase using Density Functional Theory (DFT) [59]. The functional used was B3LYP. The B3LYP method combines Becke's three parameter exchange functional (B3) [60] with the nonlocal correlation functional by Lee, Yang and Parr (LYP) [61]. The basis set used for all atoms was 6-31G (d), the latter has been justified in the literature [62, 63] for the current investigation. The vibrational frequencies at the optimized structures were computed using the same method to verify that the optimized structures correspond to local minima on the energy surface. The vertical excitation energies at the ground-state equilibrium geometries were calculated with TD-DFT [64–66]. The low-lying first singlet excited state (S_1) of each conformer was relaxed using the TD-DFT to obtain its minimum energy geometry. The difference between the energies of the optimized geometries at the first singlet excited state and the ground state was used in computing the emissions [67, 68]. The frequency computations were also carried out on the optimized geometry of the low-lying vibronically relaxed first excited state of the conformers. All the computations in solvents of different polarities were carried out using the Polarizable Continuum Model (PCM) [69, 70]. All the electronic structure computations were carried out using the Gaussian 09 program [71].

Experimental Procedure

3-(Benzo[d]oxazol-2-yl)naphthalen-2-ol (2)

A mixture of 2-aminophenol (1.09 g, 0.01 mol) and 3-hydroxynaphthalene-2-carboxylic acid 1 (1.88 g, 0.01 mol) were refluxed (133–135 °C) in chlorobenzene (10 mL) in the presence of PCl_3 (2 g, 1.3 mL, 0.01 mol) for 4 hours. After completion of reaction, the solid product was precipitated out and was filtered to get the crude product 2. Yield 2.06 g (79 %) which was further recrystallized form ethanol, mp: 171–173 °C (Lit mp: 171–172 °C) [72].

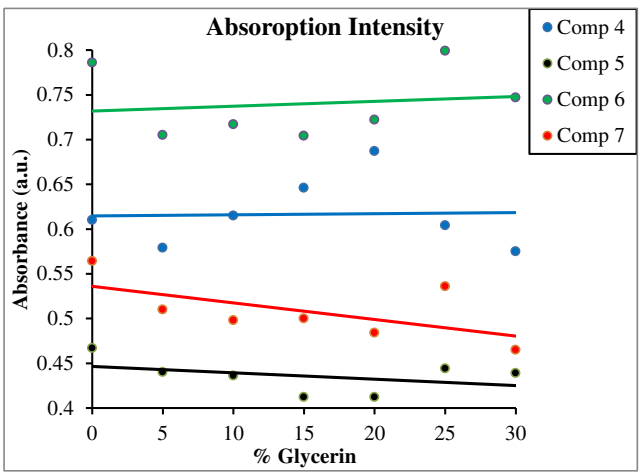

Fig. 12 Plot of absorption intensity against % of glycerin in DMF

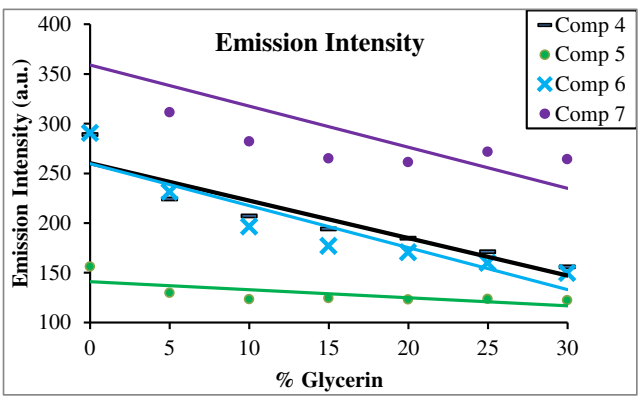

Fig. 13 Plot of emission intensity against % glycerin in DMF

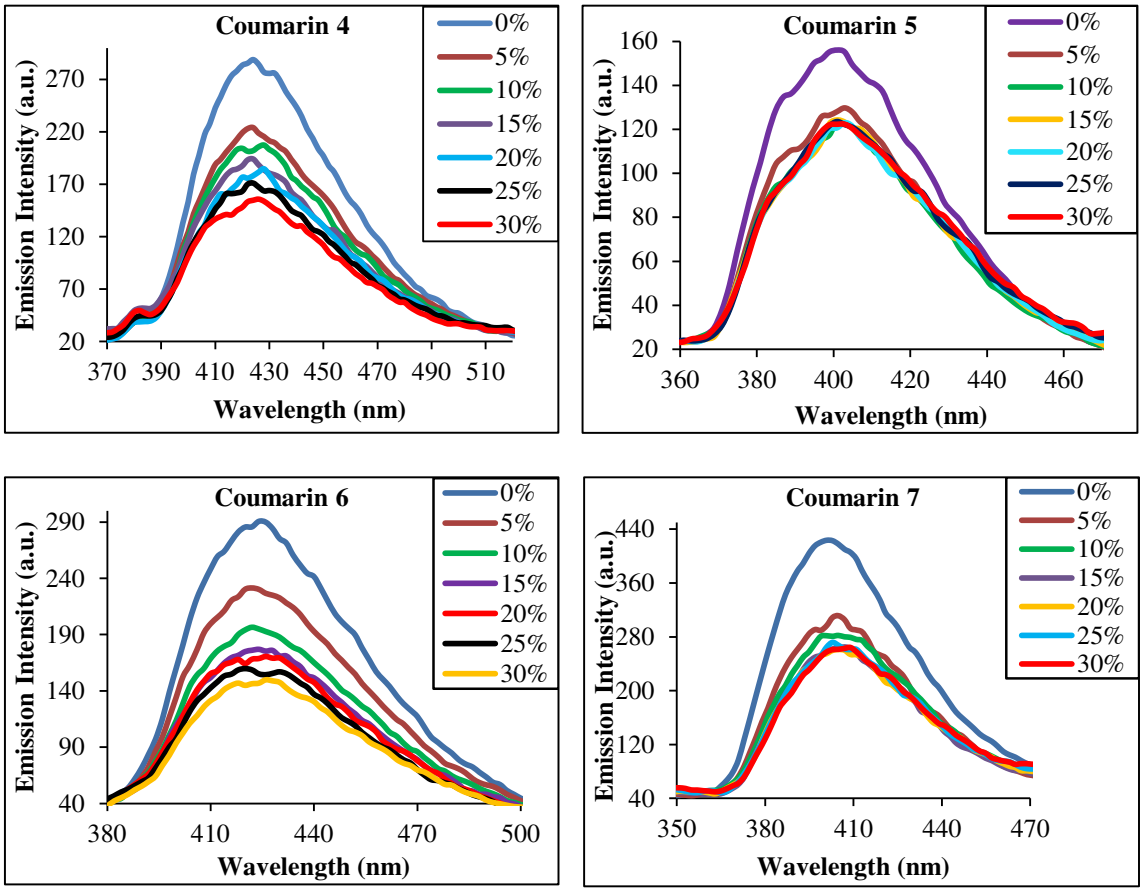

Fig. 14 Effect of viscosity on emission of coumarin 4–7

3-(1H-Benzo[d]imidazol-2-yl)naphthalen-2-ol (3)

A mixture of benzene-1, 2-diamine (1.08 g, 0.01 mol) and 3-hydroxynaphthalene-2-carboxylic acid 1 (1.88 g, 0.01 mol) was heated at 130–135 °C in stirrable amount polyphosphoric acid (5 g) for 2 h. After the completion of the reaction the tarry reaction mass was cooled to room temperature and slowly added to the crushed ice. The solid product was precipitated

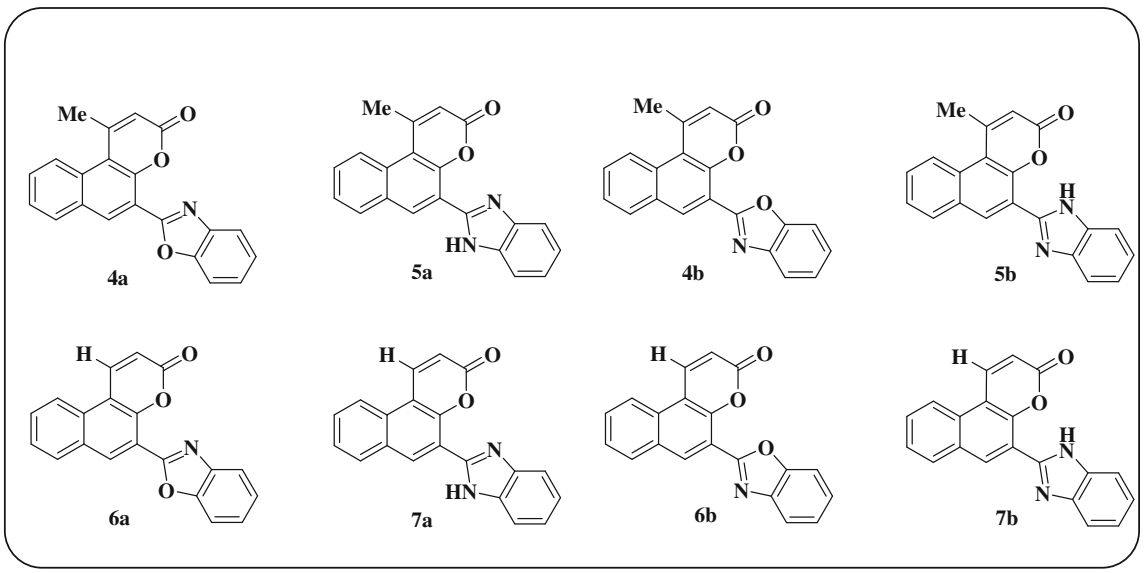

Fig. 15 The possible rotamers of coumarin 4–7

Table 2 Ground state stability of each conformer of coumarin 4–7[a]

Coumarin No	Energy (Hatree)	
	Rotamer a	Rotamer b
4	−683,049.6	−683,051.0
5	−670,584.9	−670,596.8
6	−658,382.5	−658,383.9
7	−645,918.1	−645,929.3

[a] TD-DFT computations were carried out with the use of optimized structures at B3LYP method with 6-31G (d) basis set

out, filtered and washed well with water to get the crude product 3. Yield 1.95 g (75 %) which was further recrystallized form ethanol, mp: 267–270 °C, decomp. (Lit mp: 268–272 ºC, decomp) [73].

5-(Benzo[d]oxazol-2-yl)-1-methyl-3H-benzo[f] chromen-3-one (4)

A mixture of 3-(benzo[*d*]oxazol-2-yl)naphthalen-2-ol (1.32 g, 0.005 mol) 2 and ethyl acetoacetate (0.65 g, 0.005 mol) was stirred at room temperature for 24 h in the presence of conc. H_2SO_4 (5 mL). The reaction was monitored by TLC, after the completion of the reaction the tarry reaction mass was slowly poured on crushed ice with stirring. The solid product was obtained which was filtered out and washed well with ice cold water for three to four times to get rid of the excess acidity to obtain crude product, yield: 1.17 g (71 %). Further the crude product was recrystallized from 90 % ethanol, mp:>300 ºC.

FT-IR: 3,010 (Aromatic -CH Stretching), 1,728 (C=O stretching), 1,517, 1,454, (C=C, C=N ring stretching), 1,295, 1,179 (C-O stretching), 862, 747 (Aromatic -CH out of plane bending) cm^{-1}.

^{1}H NMR: ($CDCl_3$, 300 MHz, ppm) δ=3.25 (s, 3H, CH_3), 7.35 (q, *J*=8.2 Hz, 1H, Ar-H), 7.42-7.50 (m, *J*=7.2, 8.6, 1.5 Hz, 3H, Ar-H), 7.70–7.75 (m, *J*=7.9, 2.2 Hz, 2H, Ar-H), 7.90 (dd, *J*=8.3, 7.5, 1.7 Hz, 1H, Ar-H), 8.05 (d, 8.6 Hz, 1H, Ar-H), 8.20 (dd, *J*=8.4, 2.7 Hz, 1H, Ar-H), 8.75 (d, *J*=8.5 Hz, 1H, Ar-H) ppm.^{13}C NMR: (DMSO-d_6, 125 MHz, ppm) δ= 19.8, 111.4, 113.7, 119.8, 123.0, 125.5, 125.7, 126.3, 126.5, 127.1, 127.3, 128.2, 129.7, 130.3, 132.6, 136.4, 140.1, 142.6, 153.6, 162.3 (s) ppm, Elemental analysis Calcd. for

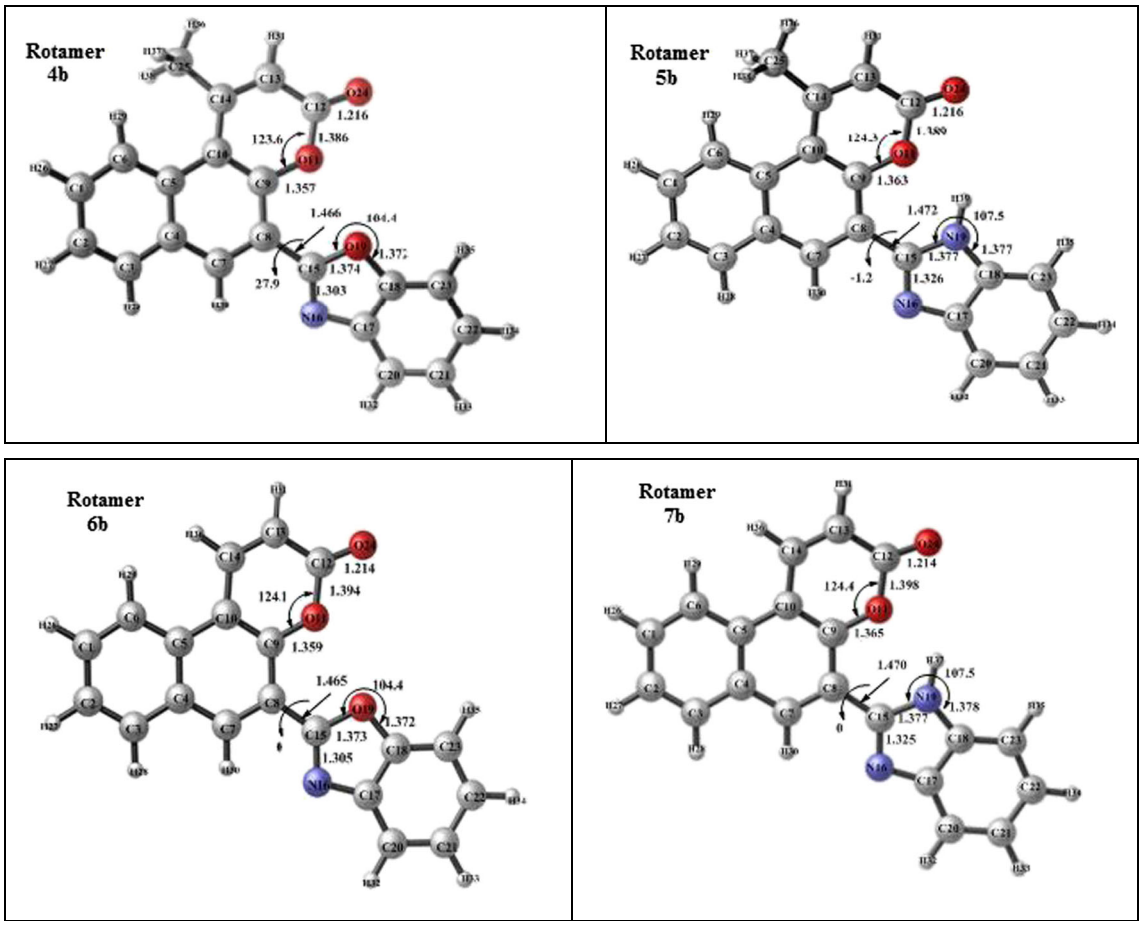

Fig. 16 Optimized structures of coumarin −4–7

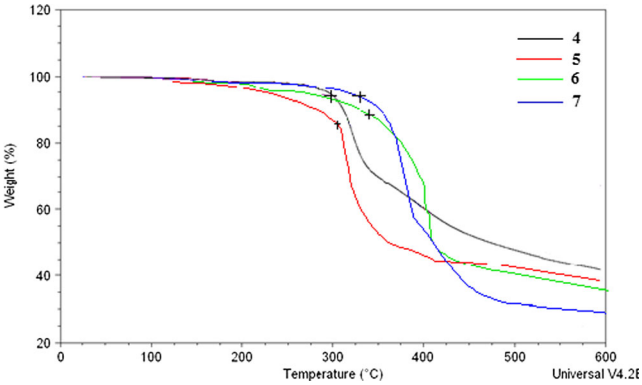

Fig. 17 TGA curves of coumarin 4–7

$C_{21}H_{13}NO3$: C 77.05, H 4.00, N 4.28 Found: C 76.98, H 3.91 and N 9.19.

5-(1H-Benzo[d]imidazol-2-yl)-1-methyl-3H-benzo[f] chromen-3-one (5)

A mixture of 3-(1H-benzo[*d*]imidazol-2-yl)naphthalen-2-ol (1.30 g, 0.005 mol) 4 and ethyl acetoacetate (0.65 g, 0.005 mol) was stirred at room temperature for 22 h in the presence of conc. H_2SO_4 (5 mL). The reaction was monitored by TLC, after the completion of the reaction the tarry reaction mass was slowly poured on the crushed ice with stirring. The solid product obtained was filtered out and washed well with ice cold water three to four times to get rid of the excess acidity to obtain the crude product, yield: 1.05 g (65 %). Further the crude product was recrystallized from 90 % ethanol, mp:>300 ºC.

FT-IR: 2,980 (Aromatic -CH Stretching), 1,725 (C=O stretching) 1,624, 1,563, 1,461, (C=C, C=N ring stretching), 1,158, 1,037 (C-O stretching), 868, 744 (Aromatic -CH out of plane bending) cm^{-1}.

^{1}H NMR: (DMSO-d_6, 300 MHz, ppm) δ=3.20 (s, 3H, CH_3), 7.35 (m, *J*=7.1, 8.5 Hz, 1H, Ar-H), 7.47–7.53 (m, *J*= 8.2, 2.4 Hz, 3H, Ar-H), 7.79 (dd, *J*=8.5, 2.3 Hz, 1H, Ar-H), 7.85–7.89 (m, *J*=7.5, 7.9, 1.8 Hz, 2H, Ar-H), 8.01 (dd, *J*=8.1, 2.2 Hz, 1H, Ar-H), 8.12 (s, 1H, NH), 8.55 (s, 1H, Ar-H), 8.72 (m, 7.2, 8.3, 1.8 Hz, 1H, Ar-H),^{13}C NMR: (DMSO-d_6, 125 MHz, ppm) δ=19.2, 111.2, 114.6, 114.8, 123.5, 125.2, 125.9, 126.3 (s), 126.5 (s), 127.3, 127.7, 128.0, 130.6, 131.7, 132.9, 136.3, 144.3, 147.8, 154.0, Elemental analysis Calcd. for $C_{21}H_{14}N_2O_2$: C 77.29, H 4.32, N 8.58 Found: C 77.12, H 4.29 and N 8.49.

5-(Benzo[d]oxazol-2-yl)-3H-benzo[f]chromen-3-one (6)

A mixture of 3-(benzo[*d*]oxazol-2-yl)naphthalen-2-ol (1.32 g, 0.005 mol) 2 and 2-hydroxysuccinic acid (0.67 g, 0.005 mol) was stirred at room temperature for 22 h in the presence of conc. H_2SO_4 (5 mL). The reaction was monitored by TLC, after the completion of the reaction the tarry reaction mass was slowly poured on the crushed ice with stirring. The solid product obtained was filtered out and washed well with ice cold water three to four times to get rid of the excess acidity to obtain the crude product, yield: 1.04 g (66 %). Further the crude product was recrystallized from 90 % ethanol, mp: 292–295 ºC.

FT-IR: 3,120 (Aromatic -CH Stretching), 1,728 (C=O stretching) 1,600, 1,563, 1,457, (C=C, C=N ring stretching), 1,180, 1,028 (C-O stretching), 864, 747 (Aromatic -CH out of plane bending) cm^{-1}.

^{1}H NMR: (DMSO-d_6, 300 MHz, ppm) δ=6.86 (d, *J*= 8.5 Hz, 1H, Ar-H), 7.32–7.34 (m, *J*=7.3, 2.7 Hz, 2H, Ar-H), 7.49 (m, *J*=7.5, 1.9 Hz, 1H, Ar-H), 7.51 (m, *J*=7.9, 1.9 Hz, 1H, Ar-H), 7.86–7.88 (m, *J*=7.6, 2.5 Hz, 2H, Ar-H), 7.91–8.00 (dd, 2H, Ar-H), 8.40 (s, 1H, Ar-H), 8.71 (s, 1H, Ar-H),^{13}C NMR: (DMSO-d_6, 125 MHz, ppm) δ=111.5, 112.2, 113.1, 119.9, 123.0 (s), 125.7 (s), 126.5 (s), 127.2, 128.2, 129.8, 130.8, 132.6, 140.2, 142.8, 149.6, 153.5, 162.3.

5-(1H-Benzo[d]imidazol-2-yl)-3H-benzo[f]chromen-3-one (7)

A mixture of 3-(1H-benzo[*d*]imidazol-2-yl)naphthalen-2-ol (1.30 g, 0.005 mol) 4 and 2-hydroxysuccinic acid (0.67 g, 0.005 mol) was stirred at room temperature for 23 h in the presence of conc. H_2SO_4 (5 mL). The reaction was monitored by TLC, after the completion of the reaction the tarry reaction mass was slowly added in to crush ice with stirring. The solid product obtained was filtered out and washed well with ice cold water three to four times to get rid of the excess acidity to obtain crude product, yield: 1.06 g (68 %). Further crude product was recrystallized from 90 % ethanol, mp:>300 ºC.

FT-IR: 2,945 (Aromatic -CH Stretching), 1,722 (C=O stretching) 1,624, 1,563, 1,459, (C=C, C=N ring stretching), 1,160, 1,037 (C-O stretching), 868, 746 (Aromatic -CH out of plane bending) cm^{-1}.

^{1}H NMR: (DMSO-d_6, 300 MHz, ppm) δ=6.86 (d, *J*=7.2 Hz, 1H, Ar-H), 7.38 (t, *J*=7.2, 1.6 Hz, 1H, Ar-H), 7.41 (m, *J*=7.1, 2.1 Hz, 1H, Ar-H), 7.51 (m, *J*=7.6, 1.2 Hz, 1H, Ar-H), 7.58 (m, *J*=7.9, 1.5 Hz, 1H, Ar-H), 7.62 (dd, *J*=8.1, 2.2 Hz, 1H, Ar-H), 7.70 (m, *J*=8.1 Hz, 1H, Ar-H), 8.59 (d, *J*=7.3 Hz, 1H, Ar-H), 8.66 (d, *J*=8.3 Hz, 1H, Ar-H), 8.76 (s, 1H, Ar-H), 8.91 (d, *J*= 8.1 Hz, 1H), 9.01 (s, 1H, NH),^{13}C NMR: (DMSO-d_6, 125 MHz, ppm) δ=111.2, 112.1, 115.2, 116.8, 123.6, 125.1 (s), 126.3 (s), 127.7, 129.1, 1,307, 131.2, 133.1, 136.4, 143.0, 144.8, 145.5, 147.3, 153.0, MS (*m*/*z*): 312.9 (M+1, 95 %).

Conclusion

To conclude, in this paper we report the synthesis of the novel fluorescent benzo[*f*]chromen-3-one (coumarin) derivatives 4–

7. All the coumarin were well characterized by ^{1}H NMR, ^{13}C NMR and mass spectroscopy. The solvatochromism study for all the molecules shows that they show absorption in the range of 314–348 nm while emit in the range of 391–572 nm. Most of the coumarin show anomalous behavior in DMF of high emission intensity with fair to good quantum yield. For all the coumarin the vertical excitations were calculated by using TD-DFT technique and they are in good correlation with the experimental absorption maxima. The largest difference between the computed absorption and the experimental absorption varies from 5 to 24 nm. The emission intensity continuously decreases as viscosity increases for all compounds. The thermogravimetric analysis shows that all the coumarin are thermally well stable up to 302–349 ºC.

Acknowledgments Kiran Phatangare is thankful to UGC-CAS for providing research fellowship under Special Assistance Programme (SAP). Sandip K. Lanke is thankful to UGG-CSIR for senior research fellowship.

References

1. De Silva AP, Gunaratne HQN, Gunnlaugsson T et al (1997) Signaling recognition events with fluorescent sensors and switches. Chem Rev 97:1515–1566
2. Berlman IB (1971) Handbook of fluorescence spectra of aromatic molecules
3. Takechi H, Kamada S, Machida M (1996) 3-[4-(Bromomethyl)phenyl]-7-(diethylamino)-2 h-1-benzopyran-2-one (mpac-br) : a highly sensitive fluorescent derivtization reagent for carboxylic acids in high-performance liquid chromatography. Chem Pharm Bull 44:793–799
4. Yu H, Zhao Q, Jiang Z et al (2010) A ratiometric fluorescent probe for cyanide: Convenient synthesis and the proposed mechanism. Sensors Actuators B Chem 148:110–116
5. Brun M-P, Bischoff L, Garbay C (2004) A Very Short Route to Enantiomerically Pure Coumarin-Bearing Fluorescent Amino Acids. Angew Chem Int Ed 43:3432–3436
6. Lin W, Long L, Tan W (2010) A highly sensitive fluorescent probe for detection of benzenethiols in environmental samples and living cells. Chem Commun 46:1503–1505
7. Hunger K (2003) Industrial dyes
8. Yamaguchi S, Akiyama S, Tamao K (2000) Photophysical properties changes caused by hypercoordination of organosilicon compounds: from trianthrylfluorosilane to trianthryldifluorosilicate. J Am Chem Soc 122:6793–6794
9. Kobiro K, Inoue Y (2002) A new chiral probe for sulfate anion: uv, cd, fluorescence, and nmr spectral studies of 1:1 and 2:1 complex formation and structure of chiral guanidinium−p-dimethylaminobenzoate conjugate with sulfate anion. J Am Chem Soc 125:421–427
10. Harvey MD, Bablekis V, Banks PR, Skinner CD (2001) Utilization of the non-covalent fluorescent dye, Nano Orange, as a potential clinical diagnostic tool: Nanomolar human serum albumin quantitation. J Chromatogr B Biomed Sci Appl 754:345–356
11. Murray RDH, Mendez J, Brown SA (1982) The natural coumarin; occurrence, chemistry and biochemistry
12. Hepworth JD (1984) Comprehensive heterocyclic chemistry. In: Katritzky AR, Rees CW (eds)Pergamon, Oxford, p 799
13. Hepworth JD, Gabbutt CD, Heron BCW (1996) Comprehensive heterocyclic chemistry-II. In: Katritzky AR, Ress CW, Scriven EF V. (eds)Pergamon, New York, p 417
14. Wang X, Krebs LJ, Al-Nuri M et al (1999) A chemically labeled cytotoxic agent: two-photon fluorophore for optical tracking of cellular pathway in chemotherapy. Proc Natl Acad Sci 96:11081–11084
15. Grynkiewicz G, Poenie M, Tsien RY (1985) A new generation of Ca2+ indicators with greatly improved fluorescence properties. J Biol Chem 260:3440–3450
16. Minta A, Kao JP, Tsien RY (1989) Fluorescent indicators for cytosolic calcium based on rhodamine and fluorescein chromophores. J Biol Chem 264:8171–8178
17. Ye D, Wang L, Li H et al (2013) Synthesis of coumarin-containing conjugated polymer for naked-eye detection of DNA and cellular imaging. Sensors Actuators B Chem 181:234–243
18. Qian Y, Yang B, Shen Y et al (2013) A BODIPY–coumarin-based selective fluorescent probe for rapidly detecting hydrogen sulfide in blood plasma and living cells. Sensors Actuators B Chem 182:498–503
19. Maity D, Karthigeyan D, Kundu TK, Govindaraju T (2013) FRET-based rational strategy for ratiometric detection of Cu2+ and live cell imaging. Sensors Actuators B Chem 176:831–837
20. Shastri L, Kalegowda S, Kulkarni M (2007) The synthesis of pyrrole bis-coumarins, new structures for fluorescent probes. Tetrahedron Lett 48:7215–7217
21. Kumar Satpati A, Kumbhakar M, Kumar Maity D, Pal H (2005) Photophysical investigations of the solvent polarity effect on the properties of coumarin-6 dye. Chem Phys Lett 407:114–118
22. Kim T-K, Lee D-N, Kim H-J (2008) Highly selective fluorescent sensor for homocysteine and cysteine. Tetrahedron Lett 49:4879–4881
23. Azim SA, Al-Hazmy SM, Ebeid EM, El-Daly SA (2005) A new coumarin laser dye 3-(benzothiazol-2-yl)-7-hydroxycoumarin. Opt Laser Technol 37:245–249
24. Christie RM (1993) Fluorescent dyes. Rev Prog Color Relat Top 23: 1–18
25. Drexhage KH (1973) Structure and properties of laser dyes, in: Dye Lasers. Topics in Applied Physics
26. Maeda M (1984) Laser Dyes. Academic Press, New York
27. Zabradnik M (1992) The production and application of fluorescent brightening agent. John Wiley and Sons, New York
28. Drexhage KH (1976) Fluorescence efficiency of laser dyes. J Res Natl Bur Stan-Phys Chem 80:421–428
29. Jones G, Jackson WR, Choi CY, Bergmark WR (1985) Solvent effects on emission yield and lifetime for coumarin laser dyes. Requirements for a rotatory decay mechanism J Phys Chem 89: 294–300
30. Culligan SW, Chen AC-A, Wallace JU et al (2006) Effect of hole mobility through emissive layer on temporal stability of blue organic light-emitting diodes. Adv Funct Mater 16:1481–1487
31. Hsu S-F, Lee C-C, Hwang S-W et al (2005) Color-saturated and highly efficient top-emitting organic light-emitting devices. Thin Solid Films 478:271–274
32. Hung LS, Chen CH (2002) Recent progress of molecular organic electroluminescent materials and devices. Mater Sci Eng: R: Reports 39:143–222
33. Christie RM, Lui C-H (2000) Studies of fluorescent dyes: part 2. An investigation of the synthesis and electronic spectral properties of substituted 3-(2′-benzimidazolyl)coumarins. Dyes Pigments 47:79–89
34. Ayyangar NR, Srinivasan KV, Daniel T (1991) Polycyclic compounds Part VII. Synthesis laser characteristics and dyeing behaviour of 7-diethylamino-2H-l-benzopyran-2-ones. Dyes Pigments 16:197–204
35. Fischer A, Cremer C, Stelzer EHK (1995) Fluorescence of coumarins and xanthenes after two-photon absorption with a pulsed titanium sapphire laser. Appl Opt 34:1989–2003

36. Moylan CR (1994) Molecular hyperpolarizabilities of coumarin dyes. J Phys Chem 98:13513–13516
37. Gordo J, Avó J, Parola AJ et al (2011) Convenient synthesis of 3-vinyl and 3-styryl coumarins. Org Lett 13:5112–5115
38. Wang Z-S, Cui Y, Hara K et al (2007) A high-light-harvesting-efficiency coumarin dye for stable dye-sensitized solar cells. Adv Mater 19:1138–1141
39. Komatsu K, Urano Y, Kojima H, Nagano T (2007) Development of an iminocoumarin-based zinc sensor suitable for ratiometric fluorescence imaging of neuronal zinc. J Am Chem Soc 129:13447–13454
40. Jagtap AR, Satam VS, Rajule RN, Kanetkar VR (2009) The synthesis and characterization of novel coumarin dyes derived from 1,4-diethyl-1,2,3,4-tetrahydro-7-hydroxyquinoxalin-6-carboxaldehyde. Dyes Pigments 82:84–89
41. Roussakis E, Pergantis SA, Katerinopoulos HE (2008) Coumarin-based ratiometric fluorescent indicators with high specificity for lead ions. Chem Commun 6221–6223
42. Pagona G, Economopoulos SP, Tsikalas GK et al (2010) Fullerene–Coumarin Dyad as a Selective Metal Receptor: Synthesis, Photophysical Properties, Electrochemistry and Ion Binding StudiesFullerene–coumarin dyad as a selective metal receptor: synthesis, photophysical properties, electrochemistry and ion bindin. Chem Eur J 16:11969–11976
43. Lee K-S, Kim T-K, Lee JH et al (2008) Fluorescence turn-on probe for homocysteine and cysteine in water. Chem Commun 6173–6175
44. Lin W, Yuan L, Cao Z et al (2009) A Sensitive and Selective Fluorescent Thiol Probe in Water Based on the Conjugate 1,4-Addition of Thiols to α, β-Unsaturated Ketones. Chem Eur J 15: 5096–5103
45. Zhao Y, Yu T, Wu Y et al (2012) Synthesis, Photo- and Electro-Luminescence of 3-Benzoxazol-2-yl-Coumarin Derivatives. J Fluoresc 22:631–638
46. Xie L, Chen Y, Wu W et al (2012) Fluorescent coumarin derivatives with large stokes shift, dual emission and solid state luminescent properties: An experimental and theoretical study. Dyes Pigments 92:1361–1369
47. Lin W, Yuan L, Cao Z et al (2010) Through-bond energy transfer cassettes with minimal spectral overlap between the donor emission and acceptor absorption: coumarin–rhodamine dyads with large pseudo-stokes shifts and emission shifts. Angew Chem Int Ed 49: 375–379
48. Hon Y-S, Tseng T-W, Cheng C-Y (2009) Electrocyclization of cis-dienals in organic synthesis: a new and versatile synthetic method for the preparation of aryl- and heteroaryl-fused coumarins. Chem Commun 5618–5620
49. Song CE, Jung D, Choung SY et al (2004) Dramatic enhancement of catalytic activity in an ionic liquid: highly practical friedel–crafts alkenylation of arenes with alkynes catalyzed by metal triflates. Angew Chem Int Ed 43:6183–6185
50. Signore G, Nifosì R, Albertazzi L et al (2010) Polarity-sensitive coumarins tailored to live cell imaging. J Am Chem Soc 132:1276–1288
51. Fadda AA, Refat HM, Zaki MEA (2000) Utility of sulphones in heterocyclic synthesis: synthesis of some pyridine, chromene and thiophene derivatives. Molecules 5:701–709
52. Padalkar V, Tathe A, Gupta V et al (2012) Synthesis and photophysical characteristics of ESIPT inspired 2-substituted benzimidazole, benzoxazole and benzothiazole fluorescent derivatives. J Fluoresc 22:311–322
53. Patil VS, Padalkar VS, Phatangare KR et al (2011) Synthesis of new ESIPT-fluorescein: photophysics of pH sensitivity and fluorescence. J Phys Chem A 116:536–545
54. Gupta VD, Padalkar VS, Phatangare KR et al (2011) The synthesis and photo-physical properties of extended styryl fluorescent derivatives of N-ethyl carbazole. Dyes Pigments 88:378–384
55. Phatangare KR, Patil AB, Patil VS et al (2012) Synthesis, photophysical properties of novel fluorescent metal complexes from 3-(1,3-benzoxazol-2-yl)naphthalen-2-ol, and their antimicrobial activity. Curr Chem Lett 1:47–58
56. Phatangare KR, Gupta VD, Tathe AB et al (2013) ESIPT inspired fluorescent 2-(4-benzo[d]oxazol-2-yl)naphtho[1,2-d]oxazol-2-yl)phenol: experimental and DFT based approach to photophysical properties. Tetrahedron 69:1767–1777
57. Williams ATR, Winfield SA, Miller JN (1983) Relative fluorescence quantum yields using a computer-controlled luminescence spectrometer. Analyst 108:1067–1071
58. Dhami S, De Mello AJ, Rumbles G et al (1995) Phthalocyanine fluorescence at high concentration: dimers or reabsorption effect? Photochem Photobiol 61:341–346
59. Treutler O, Ahlrichs R (1995) Efficient molecular numerical integration schemes. J Chem Phys 102:346–354
60. Becke AD (1993) A new mixing of Hartree–Fock and local density functional theories. J Chem Phys 98:1372–1377
61. Lee C, Yang W, Parr RG (1988) Development of the Colle-Salvetti correlation-energy formula into a functional of the electron density. Phys Rev B 37:785–789
62. Casida ME, Jamorski C, Casida KC, Salahub DR (1998) Molecular excitation energies to high-lying bound states from time-dependent density-functional response theory: Characterization and correction of the time-dependent local density approximation ionization threshold. J Chem Phys 108:4439–4449
63. Kim CH, Park J, Seo J et al (2010) Excited state intramolecular proton transfer and charge transfer dynamics of a 2-(2′-hydroxyphenyl)benzoxazole derivative in solution. J Phys Chem A 114:5618–5629
64. Hehre WJ, Radom L, Schleyer PV, Pople J (1986) Ab Initio Molecular Orbital Theory. Wiley, New York
65. Bauernschmitt R, Ahlrichs R (1996) Treatment of electronic excitations within the adiabatic approximation of time dependent density functional theory. Chem Phys Lett 256:454–464
66. Furche F, Rappaport D (2005) Density functional theory for excited states: Equilibrium structure and electronic spectra. In Computational Photochemistry
67. Lakowicz JR (1999) Principles of Fluorescence Spectroscopy, 2nd edn. Kluwer Academic, New York
68. Valeur B, Berberan-Santos MN (2001) Molecular fluorescence: principles and applications. Wiley-VCH Verlag, Weinheim
69. Cossi M, Barone V, Cammi R, Tomasi J (1996) Ab initio study of solvated molecules: a new implementation of the polarizable continuum model. Chem Phys Lett 255:327–335
70. Tomasi J, Mennucci B, Cammi R (2005) Quantum mechanical continuum solvation models. Chem Rev 105:2999–3094
71. Frisch MJ, Trucks GW, Schlegel HB, et al. (2009) Gaussian 09, Revision C.01. Gaussian 09, Revision B01, Gaussian, Inc, Wallingford CT
72. Ueno R, Kitayama Y, Minami K, Wakamori H (2004) Binaphthol derivative and process for producing the same
73. Douhal A, Amat-Guerri F, Acuña AU, Yoshihara K (1994) Picosecond vibrational relaxation in the excited-state proton-transfer of 2-(3′-hydroxy-2′-naphthyl)benzimidazole. Chem Phys Lett 217:619–625